

Plasma slab expansion into a vacuum: from quasineutral outflow to Coulomb explosion

V. Yu. Bychenkov^{1,2}, E. A. Govras^{1,2}

¹ *P.N. Lebedev Physical Institute, Moscow, Russia*

² *All-Russia Research Institute of Automatics, Moscow, Russia*

Ion acceleration during plasma expansion into vacuum was first studied by Gurevich et al. [1]. Important qualifying step was taken by Mora in Ref. [2] where the ion front was studied in details. These works considered a semi-infinite plasma. Both of them are widely applied to laser triggered ion acceleration. However, only ultrathin plasma foils are able to provide high ion energy [3, 4] that stress a lack of analytical models of expansion of thin plasma layer into a vacuum. Our work takes a step forward in closing this gap.

Initially homogeneous plasma slab of thickness L with ion charge Ze , mass M , and density n_0 is in the region $-L/2 \leq x \leq L/2$. Plasma expansion is governed by the Vlasov equation for ions with self-consistent field $E(x, t)$ described by the Poisson equation and the electron density which follows the Boltzmann distribution with given temperature T . Such a description is so called kinetic Boltzmann-Vlasov-Poisson (BVP) model [5]. The corresponding system of equations which describes plasma expansion in a vacuum is:

$$\begin{aligned} \ddot{x} &= -\varphi'(x, t), \quad x(0) = x_0, \dot{x}(0) = 0, \quad n(x, t) = \left| \frac{\partial x(x_0, t)}{\partial x_0} \right|^{-1}, 0 \leq x_0 \leq 1 \\ \varphi'' &= \eta^e \exp \left[\frac{\varphi}{T} \right] - n(x, t), \quad \varphi'|_{x=0} = \varphi'|_{x=\infty} = 0. \end{aligned} \quad (1)$$

In Eqs.(1) due to a symmetry we consider $x \geq 0$ and the following units: $L/2$ for coordinates, x ; $\omega_{pi}^{-1} = \sqrt{M/4\pi(Ze)^2 n_0}$ for time, t ; n_0 for ion density, n ; $4\pi(Ze)^2 n_0 (L/2)^2$ for energies, $(Ze\varphi, ZT$ or $\epsilon = M\dot{x}^2/2$). Dimensionless parameter η^e describes initial electron depletion of the target, $\eta^e = n_0^e/Zn_0$, and can be approximately found: $\eta^e = 1/(1 + 2T)$.

So far solution of Eqs.(1) was restricted by the numerical simulation (e.g., the PIC algorithm) because of complicated self-consistent calculation of the ion density $n(x, t)$. The other approximate way is to apply a model ion density from the following physical arguments. Coulomb explosion (CE) of plasma slab [6] is relevant to high electron energies ($T \gg 1$). It is accompanied by homogeneity of the ion density profile: $n(x, t) = 1/x_f(t)$, with $x_f(t)$ to be the front position of expanding ion plasma. On the other hand, weakly heated plasma expands in quasineutral regime [1]: $n(x, t) \approx n^e(x, t) = \eta^e \exp[\varphi/T]$. By using these asymptotics we may propose a

simple density fit to generalize known limiting expressions for $n(x, t)$ to arbitrary T :

$$n(x, t > 0) = \left\{ \eta^e \exp \left[\frac{\varphi(x, t)}{T} \right] \cdot A + \frac{1}{x_f(t)} \cdot B \right\} \cdot \theta(x_f(t) - x), \quad (2)$$

where $\theta(x)$ is the Heaviside step function. The interpolation coefficient A describes smooth transition from the quasineutral regime to the CE, i.e. $A(T \rightarrow 0) \rightarrow 1$ and $A(T \rightarrow \infty) \rightarrow 0$. The coefficient B uniquely follows from A due to the density normalization ($\int_0^{x_f} n(x, t) \equiv 1$):

$$B = 1 - A + A \sqrt{2 \eta^e T e^{-\delta(t)} \exp[\varphi_0(t)/T]}, \quad (3)$$

where $\varphi_0(t)$ is the plasma potential at the slab center ($x = 0$) and $\delta(t)$ is the potential difference in a plasma, $\delta(t) = [\varphi_0(t) - \varphi_f(t)]/T$. By choosing the simplest form, $A(T) = 1/(1 + T)$, one obtains the following expressions for the field at the ion front:

$$E_f = \frac{2 T \delta e^{-\delta/2}}{x_f} \sqrt{\frac{1 + T}{T(1 - \delta) + e^{-\delta}}}, \quad \text{where} \quad (4)$$

$$2 e^{\delta/2} (T + e^{-\delta}) \sqrt{1 + T} = \left[1 + \sqrt{1 + 2 x_f e^\delta (T + e^{-\delta}) / \delta} \right] \cdot \sqrt{T(1 - \delta) + e^{-\delta}}. \quad (5)$$

The first integral of the front motion equation $\ddot{x}_f = E_f$ with E_f from Eq. (4) provides a quadrature formula for the ion maximum energy

$$\epsilon_{max}(x_f, T) = 2 T \sqrt{1 + T} \int_1^{x_f} \frac{\delta e^{-\delta/2}}{x \sqrt{T(1 - \delta) + e^{-\delta}}} dx. \quad (6)$$

In accordance with Ref. [2], the electric field at the ion front $E_f = 2 \sqrt{4 \pi T Z n_0 / (2 e + \omega_{pi}^2 t^2)}$ for the semi-infinite plasma reads (in our dimensionless units):

$$E_f^{[2]} = \frac{2 \sqrt{T}}{\sqrt{2 e + t^2}}. \quad (7)$$

In Fig. 1 we compare numerical and approximate analytical solutions for E_f . Note that, $E_f = 1$ corresponds to the CE regime ($T \rightarrow \infty$). Whereas analytic solution (4) demonstrates excellent agreement with the numerical one, the solution (7) deviates from both of them if temperature does not follow the condition $T \ll 1$. Exterior to applicability condition, $T > 1$, the solution (7) unphysically exceeds the maximum possible field which corresponds to the CE [6], $E_f^{CE} \equiv 1$. For small electron temperature, $T \ll 1$, i.e. for small the electron Debye length to the foil thickness ratio $\lambda_D^e / L \lesssim 1$, both Eq.(7) and (4) are in close agreement.

One-dimensional approach corresponds to infinite electrostatic energy of a slab. Thus, ion maximum energy infinitely increases with time. In order to make an adequate estimates we

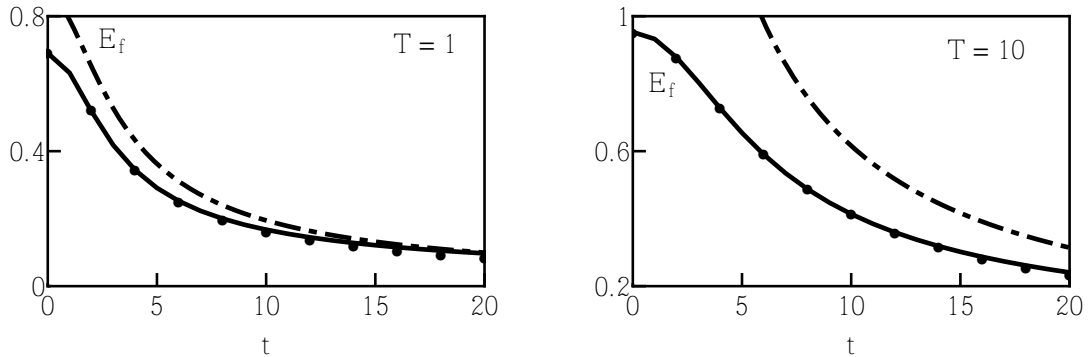


Figure 1: Evolution of the electric field at the ion front from Eq.(4) (solid curves) in comparison with Eq.(7) (dot-dashed lines) and the BVP numerical result with PIC method (solution to Eqs.(1), dots).

restrict one-dimensional consideration when a plasma expands at a distance approximately equal to the radius of the laser focal spot, R_f , [6]. At $x > R_f$ the three-dimensional effects significantly decrease accelerating fields, so the ions gain the main part of resultant energy during one-dimensional stage. This is why we introduce "virtual detector", the plane with coordinate $x_d = R_f$, which registers energy of the arriving particles. The ion energy at this "virtual detector" models energy of the ions at a real detector. For relevant experimental conditions with ultrathin foils, which provide efficient ion acceleration a foil thickness can vary on length scale of tens or hundreds of nanometers [7, 8] and focal spot radius is of the order of few laser wavelengths. Hence, typically x_d is of a few dozens. Figure 2 shows the temperature dependence of the maximum ion energy at the detector at $x_d = 20$. Our approximate analytic solution (6) demonstrates good agreement with numerical one over the entire temperature range unlike Eq.(7) which is applicable only for small values of T .

Finally, we demonstrate how laser parameters can be introduced in our analytical theory to derive ion energy dependencies on laser power and spot size. Figure 3 shows dependence of maximum ion energy per nucleon on laser focal spot radius calculated from Eq.(6) by using electron temperature scaling [9]: $T = mc^2(\sqrt{1 + A_{abs} \cdot a^2/2} - 1)$ and optimum foil thickness [10, 11]: $L \simeq (n_{cr}/Zn_0)a\lambda/\pi$. Here $a = 0.85\sqrt{I10^{-18}\lambda^2}$ is the dimensionless amplitude of a

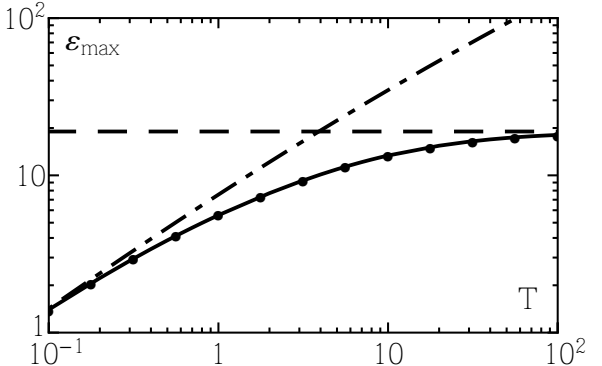


Figure 2: Temperature dependence of the maximum ion energy at the detector from Eq.(6) (solid curve) in comparison with the numerical BVP result (dots), the energy for CE ($\epsilon_{max}^{CE} = x_d - 1$) (dashed line), and Eq.(7) (dot-dashed curve).

laser field with intensity I W/cm² and wavelength λ μm , A_{abs} is the absorbtion coefficient, and n_{cr} is the electron critical density. Note, that sharp laser-plasma interface facilitates significant reflection of the light and optimum target thickness corresponds to plasma relativistic semi-transparency, i.e. significant part of laser energy is lost during laser plasma interaction ($A_{abs} < 1$). Pulse length τ is assumed to be not less than acceleration time, so that ions reach the "virtual detector" before the pulse ends and electrons start to cool down. For given laser power, increase of a focal spot size decreases an laser intensity and electron temperature. Correspondingly, the ion energy decreases. However, focal spot size increase also increases acceleration length that is favorable for ion energy gain. Competition between these effects may result in optimum spot size that is seen in Fig. 3 for 1 PW case near the diffraction limit ($R_f \simeq 1\mu\text{m}$) of the focused laser beam.

The work was partly supported by the Russian Foundation for Basic Research (grants 12-02-31183-mol_a, 12-02-33045-mol_a_ved, 12-02-00231-a, 13-02-00426_a) and The Ministry of education and science of Russian Federation (project # 8690).

References

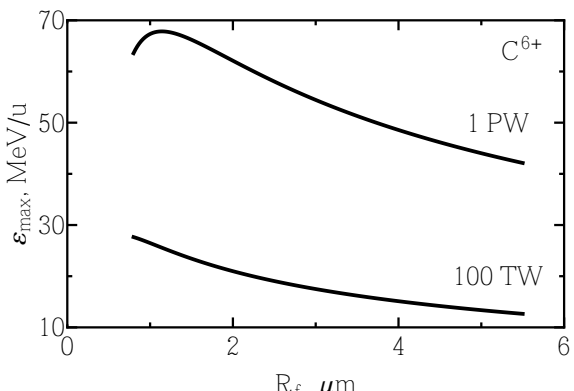


Figure 3: Maximum ion energy per nucleon from the semi-transparent diamond-like carbon foil of optimum thickness versus laser focal spot radius for 100 TW and 1 PW laser pulses ($A_{abs} = 50\%$).

- [1] A.V. Gurevich, L.V. Pariiskaya, L.P. Pitaevskii, Sov. Phys. JETP **22**, 449 (1966)
- [2] P. Mora, Phys. Rev. Lett. **90**, 185002 (2003)
- [3] A.J. Mackinnon, M. Borghesi, S. Hatchett, Phys. Rev. Lett. **86**, 1769 (2001)
- [4] Y. Sentoku, V.Yu. Bychenkov, K. Flippo et al., Appl. Phys. B **74**, 207 (2002)
- [5] V.Yu. Bychenkov, V.N. Novikov, D. Batani et al., Phys. Plasmas **11**, 3242 (2004).
- [6] V.Yu. Bychenkov, V.F. Kovalev, Quantum Electronics **35**, 1143 (2005)
- [7] A. Brantov, V.Yu. Bychenkov, D.V. Romanov et al., Contrib. Plasma Phys. **53**, 161 (2013).
- [8] D. Jung, L. Yin, B.J. Albright, et. al. New J. Phys. **15**, 023007 (2013)
- [9] S.C. Wilks, W.L. Kruer, M. Tabak, et al., Phys. Rev. Lett. **69**, 1383 (1992)
- [10] T. Esirkepov, M. Yamagiwa, T. Tajima, Phys. Rev. Lett. **96**, 105001 (2006)
- [11] A.V. Brantov, V.Yu. Bychenkov, W. Rozmus, Quantum Electronics **37**, 863 (2007)